ISSN 1063-7761, Journal of Experimental and Theoretical Physics, 2023, Vol. 137, No. 4, pp. 533–541. © Pleiades Publishing, Ltd., 2023.
Russian Text © The Author(s), 2023, published in Zhurnal Eksperimental'noi i Teoreticheskoi Fiziki, 2023, Vol. 164, No. 4, pp. 615–625.

Role of Vacancies in the Yao–Lee Model

V. A. Polyakov[a,*] and N. B. Perkins[b,]**

[a] *Moscow Institute of Physics and Technology (National Research University), Dolgoprudny, Moscow oblast, 141701 Russia*

[b] *School of Physics and Astronomy, University of Minnesota, Minneapolis, MN, 55455 USA*

**e-mail: polyakov.va@phystech.edu*

***e-mail: nperkins@umn.edu*

Received June 17, 2023; revised June 25, 2023; accepted June 25, 2023

Abstract—We consider the effect of vacancies on the low-energy excitation spectrum of a quantum spin liquid realized in the exactly solvable Yao–Lee model [H. Yao and D.-H. Lee, Phys. Rev. Lett. **107**, 087205 (2011)]. Physically, vacancies can appear for different reasons (e.g., because of zero magnetic moments on the lattice, or the presence of nonmagnetic impurities, or a random reduction of local bonds of magnetic moments with the remaining lattice). It is shown numerically that the finite density of random vacancies in this model leads to the accumulation of states near zero energy, which can be detected from the change of the behavior of heat capacity at low temperatures. Moreover, it is shown that the low-energy modes are localized more strongly than remaining eigenmodes. This effect is illustrated using the inverse participation ratio (IPR). In the case of time reversal symmetry breaking (e.g., due to the presence of a magnetic field), a gap is opened in the fermion spectrum of the model, and vacancy-induced localized states appear. The energies of these states depend on the structure of the interactions responsible for the time inversion symmetry breaking.

DOI: 10.1134/S1063776123100084

1. INTRODUCTION

Recent investigations have revealed that topology, frustration, and disorder are the key factors for the emergence of peculiar phases of matter in solid-state systems with a strong spin–orbit interaction [2]. In weakly correlated systems, the spin–orbit interaction leads to the realization of topologically nontrivial states, among which a topological insulator is one of the most striking examples [3–5]. In strongly correlated systems (so-called Mott insulators), a quantum spin liquid (QSL) can be realized.

Quantum spin liquids were predicted theoretically by Anderson in 1973 [6]. A quantum spin liquid possesses peculiar properties. Magnetic moments (spins) in QSLs are disordered, and all of them are entangled with one another in the ground state. In other words, the spin direction at a site depends on the spin direction at another site irrespective of the distance between them. Moreover, magnetic excitations in QSLs carry a spin of 1/2 (i.e., are fermions). Quantum entanglement and the fractional nature of elementary excitations impart interesting properties to QSLs. For this reason, various models realizing QSLs attract considerable attention and are actively investigated [6–12]. For example, the spin–orbit interaction and strong correlations between electrons make it possible to realize the Kitaev model on a hexagonal lattice [13]. This model is of special importance as the first exactly solvable QSL model in two dimensions [13]. At present, other models with exact solution, the ground state of which is a QSL, are also known [1, 14–18].

A spin liquid is a very rare magnetic state of matter, and not a single substance has been found, which can be unambiguously treated as a QSL. Nevertheless, many magnetic materials have been obtained in recent years, which can apparently be adequately described by QSL models. Such materials are actively investigated experimentally [9, 11, 12]. In some of such materials (mainly in compounds of transition metals with a strong spin–orbit interaction and the corresponding three-coordinate geometry [19, 20]), the Kitaev interaction appears, in which spin components of only one type are interacting on each edge of the lattice. This makes it possible to study the properties of a Kitaev QSL in actual materials [13].

Unfortunately, a direct experimental observation of QSL is quite problematic since the absence of the long-range magnetic order does not mean that the ground state of the system is a spin liquid. For example, the absence of the long-range order in the system can be due to its disorder, and since absolutely pure materials do not exist in nature, it is important to find out whether the spin ordering suppression is due to intrinsic properties of a QSL or is associated with disorder in the system.

The disorder effect were studied in the Kitaev QSL [21–28], and it was shown that in may respects they resemble localization of electronic states in the presence of disorder [29, 30]. This is due to the fact that the fermionic quasiparticles describing excitations in the Kitaev QSL even in the presence of frozen-in disorder remain noninteracting and, hence, the ideas of the Anderson localization are inapplicable [29]. Moreover, the fact that the Kitaev model with disorder remains exactly solvable makes it possible to perform direct numerical calculations. It has been shown in previous publications that a low vacancy concentration generally preserves the spin-liquid behavior in the Kitaev model, but leads to certain changes in its low-energy spectrum [25, 26, 28]. In particular, the Majorana states associated with vacancies form a peak in the density of states at low energies; the shape of this peak is successfully described by a power law. In addition, the states within this peak are more localized than other states in the system [26]. The localization of low-energy states is especially strong when the time inversion symmetry is broken by the three-particle interaction, which is an effect of the external magnetic field. A different situation takes place in the Kitaev QSL with disorder in bonds [23], where localization occurs not at low, but at high energies, forming the so-called Lifshitz tails [30].

This study is aimed at analysis of low-energy quasi-localized Majorana states that appear in the Yao–Lee model [1] in the presence of vacancies. The Yao–Lee model is exactly solvable, and its ground state is a QSL [1]. At present, there is no material that can be described by this model; however, the possibility of obtaining in future the Kitaev interactions between $J_{\text{eff}} = 3/2$ in 2D Van der Waals magnets [40] is an experimental motivation for studying the nature of this exotic QSL. The Yao–Lee model has not only the spin degrees of freedom, but also additional local orbital degrees of freedom, which, analogously to the Kitaev model, can be represented using Majorana fermions [1]; however, in contrast to the Kitaev model, its fermion representation includes three types of Majorana fermions.

The Yao–Lee model exhibits gauge symmetry Z_2 with Z_2 flux excitations that are determined exclusively in terms of the orbital degrees of freedom. When the time reversal symmetry (TRS) is broken, each type of the Majorana fermions behaves as a Bogoliubov quasiparticle in a chiral ($p + ip$) superconductor [1]. As a result, each Z_2 flux operator connects three zeroth Majorana modes protected by the SU(2) symmetry. In this article, we demonstrate that like in the Kitaev model with disorders at sites [21, 22, 25], a vacancy leads to the emergence of a mode with zero energy and a quasi-localized wavefunction at the boundary of the packet associated with it (on another sublattice around a vacancy), which is called the p mode. In addition, when TRS is not broken or when the external field violating it is weak, the vacancy and the Z_2 flux form a bound state. Therefore, in the case of TRS breaking, a vacancy acquires a topologically protected zero-energy mode, known as the f mode. The number of such topological modes depends on the type of interaction breaking TRS: if it preserves the SU(2) symmetry, we have three Majorana modes with zero energy; however, if the interaction violates this symmetry, the number of zero-energy modes is smaller.

2. DESCRIPTION OF THE MODEL

The Yao–Lee model [1] is defined on a hexagonal lattice in which each site is formed by three connected vertices (Fig. 1),

$$H_{YL} = \tilde{J}\sum_i \mathbf{S}_i^2 + \sum_{\langle ij\rangle_\lambda} J_{ij}^\lambda [\tau_i^\lambda \tau_j^\lambda][\mathbf{S}_i \mathbf{S}_j], \tag{1}$$

where the summation is performed over all vertices of the hexagonal lattice, which are denoted by i, j; $\mathbf{S}_i = \mathbf{S}_{i,1} + \mathbf{S}_{i,2} + \mathbf{S}_{i,3}$ is the total spin of each triangle, and operators τ_i^λ describing the orbital degrees of freedom are defined as

$$\tau_i^x = 2(\mathbf{S}_{i,1}\mathbf{S}_{i,2} + 1/4),$$

$$\tau_i^y = 2(\mathbf{S}_{i,1}\mathbf{S}_{i,3} - \mathbf{S}_{i,2}\mathbf{S}_{i,3})/\sqrt{3},$$

$$\tau_i^z = 4\mathbf{S}_{i,1} \cdot (\mathbf{S}_{i,2} \times \mathbf{S}_{i,3})/\sqrt{3}.$$

If $\tilde{J} \gg J^\lambda$, assuming that all the bonds J^λ have the same interaction strength, we can consider only the states with the total spin

$$\mathbf{S} = \frac{1}{2}\boldsymbol{\sigma},$$

on each triangle, where τ_i^λ denote the Pauli spin matrices. In such a situation, the first term in expression (1) is constant, while the second term can be written as

$$H = \frac{1}{4}\sum_{\langle ij\rangle_\lambda} J_{ij}^\lambda [\tau_i^\lambda \tau_j^\lambda][\boldsymbol{\sigma}_i \boldsymbol{\sigma}_j]. \tag{2}$$

Analogously to the Kitaev model [13], it is convenient to express the spin operators in terms of the Majorana fermions in the extended Hilbert space so that the spin and orbital operators are represented as [1]:

$$\boldsymbol{\sigma}_i = -i\mathbf{c}_i \times \mathbf{c}_i, \quad \boldsymbol{\tau}_i = -i\mathbf{d}_i \times \mathbf{d}_i. \tag{3}$$

Here, we have used the vector notation for the Majorana fermions,

$$\mathbf{c}_i = (c_i^x, c_i^y, c_i^z), \quad \mathbf{d}_i = (d_i^x, d_i^y, d_i^z),$$

with the commutation relations defined as

$$\{c_i^\alpha, c_j^\beta\} = \{d_i^\alpha, d_j^\beta\} = \delta_{ij}\delta_{\alpha,\beta},$$

$$\{c_i^\alpha, c_j^\beta\} = 0.$$

It is convenient to express the Pauli matrices in terms of the Majorana fermions:

$$\sigma_i^\alpha \tau_i^\beta = ic_i^\alpha d_i^\beta,$$
$$\sigma_i^\alpha = -\frac{\epsilon^{\alpha\beta\gamma}}{2} ic_i^\beta c_i^\gamma, \quad (4)$$
$$\tau_i^\alpha = -\frac{\epsilon^{\alpha\beta\gamma}}{2} id_i^\beta d_i^\gamma.$$

Substituting these expression into (2), we obtain the Hamiltonian in terms of Majorana fermions $\mathbf{c}_i$ with coupling operators $\hat{u}_{ij} = -id_i^\lambda d_j^\lambda$:

$$H = \frac{1}{4}\sum_{\langle ij\rangle_\lambda} J_{ij}^\lambda \hat{u}_{ij}(i\mathbf{c}_i\mathbf{c}_j). \quad (5)$$

This Hamiltonian describes three types of noninteracting Majorana fermions c_i^κ, $\kappa = x, y, z$, which are connected with Z_2 gauge field $\hat{u}_{ij}$. Operators $\hat{u}_{ij}$ are the first integrals of this Hamiltonian. Therefore, $u_{ij} = \pm 1$. In addition, Hamiltonian (5) has global symmetry SO(3), which is associated with the rotation in the space of three types of Majorana fermions, and is a consequence of the SU(2) symmetry of initial spin model (1). In accordance with the Lieb theorem [41], as well as in the Kitaev model [13], the ground state has zero flux through each cell p, i.e., $W_p = \Pi_{ij} u_{ij} = 1$ (if $W_p = \Pi_{ij} u_{ij} = -1$, we assume that the flux is present). Each set W_p corresponds to several sets of $\{u_{ij}\}$ differing in the gauge transformation that does not change the Hamiltonian. We assume that the gauge $u_{ij} = 1$ on all edges corresponds to zero fluxes in the ground state. Further, all three Majorana fermions have the same dispersion for any flux distribution, i.e., the fermion spectrum is three-fold degenerate in the entire Brillouin zone. In the case of zero flux in the ground state, their dispersions are identical to those obtained in the Kitaev model [13], i.e., they are either gapless with a linear dispersion, or have a gap depending on the relation between parameters J_λ:

$$\varepsilon_{\mathbf{k}}^\kappa = \sum_{\lambda=x,y,z} J^\lambda e^{i\mathbf{k}\cdot\hat{\mathbf{r}}_\lambda},$$

where $\hat{\mathbf{r}}_{x,y,z}$ denotes the vector directed from any vertex in sublattice A to its nearest neighbors in sublattice B.

2.1. Time Reversal Symmetry Breaking

TRS breaking usually occurs in a nonzero magnetic field. The problem with a magnetic field, which is included into the Hamiltonian in the form of the Zeeman interaction, cannot be solved exactly because the inclusion of the field does conserve fluxes. However, one can still add to the Hamiltonian the interaction that breaks TRS and imitates the effect of the magnetic field, but preserves the exact solvability of the model. Following Kitaev's idea [13], we apply the perturbation theory to the ground state with zero flux and obtain the effective Hamiltonian in a fixed gauge, which can be represented as before in terms of Majorana fermions $\mathbf{c}_i$ and operators $\hat{u}_{ij}^\lambda = -id_i^\lambda d_j^\lambda$.

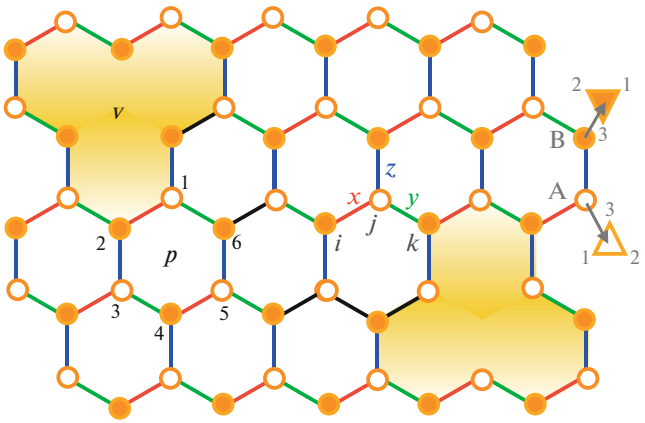

Fig. 1. Schematic diagram of the Yao–Lee model in the form of a hexagonal lattice in which three spins are located equidistantly on each site (at the vertices of triangles); the spins are coupled by the exchange Ising interactions J^λ. Three types J^x, J^y, and J^z of the Ising interaction at bonds x, y, and z are shown by red, green, and blue lines, respectively. Triangles are denoted by letters i and j; the vertices inside each triangle are denoted by 1, 2, and 3. Letters v and p denote the vacancy center and the center of the hexagon, on which operators W_v and W_p are defined, respectively. A pair of vacancies with a flux attached to each of them is formed in accordance with the following scheme: (i) a pair of adjacent vacancies is randomly placed on the lattice; (ii) the sign of variable u_{ij} on the common bond changes from $u = +1$ to $u = -1$ (black line) so that the two fluxes are produced and attached to two vacancy plaquettes; (iii) one of vacancies in a pair moves at random direction and, simultaneously, the chain of variables u_{ij} changes sign so that the fluxes are always attached to the moving vacancy.

Let us consider the isotropic Kitaev interaction $J^x = J^y = J^z = J$ and write the perturbation in form

$$V = \sum_i (h_x\tau_i^x + h_x\tau_i^x + h_x\tau_i^x) + K\sum_{\langle ik\rangle} \boldsymbol{\sigma}_i\boldsymbol{\sigma}_k, \quad (6)$$

It can easily be seen that only in the fourth order of perturbation theory fluxes through hexagonal cells are unchanged, while TRS is is broken. The fourth order correction to the Hamiltonian must contain three terms with h and one more term with K:

$$H^{(4)} = 3!\sum_{ijk} \frac{Kh_xh_yh_z}{\Delta_{jk}\Delta_{jk}\Delta_k}(\boldsymbol{\sigma}_i\boldsymbol{\sigma}_k)\tau_i^x\tau_j^z\tau_k^y, \quad (7)$$

where Δ_k is the energy change after the application of the operator τ_k^y, and Δ_{jk} is the energy change after the application of the operator $\tau_j^z\tau_k^y$.

Another (more general) form of perturbation (6) is

$$V = \sum_i (h_x\tau_i^x + h_x\tau_i^x + h_x\tau_i^x) + \sum_{\langle\langle ik\rangle\rangle}\sum_{\lambda,\mu} K^{\lambda\mu}\sigma_i^\lambda\sigma_k^\mu. \quad (8)$$

Here, $K_{\lambda\mu}$ includes all nondiagonal terms allowed by symmetry. Assuming that

$$K^{\lambda\mu} = K\delta_{\lambda\mu} + (1-\delta_{\lambda\mu})K',$$

and using the Majorana representation for spins σ and pseudospins τ, we can write the perturbed Hamiltonian as

$$H = \sum_{\langle ij\rangle}\sum_\lambda iJ_{ij}^\lambda \hat{u}_{ij}c_i^\lambda c_j^\lambda + \sum_{\langle\langle ik\rangle\rangle}\sum_\lambda i\kappa\hat{u}_{ij}\hat{u}_{jk}c_i^\lambda c_k^\lambda + \sum_{\langle\langle ik\rangle\rangle} i\eta\hat{u}_{ij}\hat{u}_{jk}\sum_{\lambda\neq\mu} c_i^\lambda c_k^\mu, \quad (9)$$

where $\langle ij\rangle$ and $\langle\langle ik\rangle\rangle$ denote the nearest and next to nearest neighbors, respectively, and $\kappa \sim 6\dfrac{Kh_xh_yh_z}{J^3}$ and $\eta \sim 6\dfrac{K'h_xh_yh_z}{J^3}$ (here, we have taken advantage of the fact that the flux energy is proportional to binding strength $J_{ij}^\lambda \equiv J$, like in the Kitaev model [13]).

2.2. Majorana Fermion Spectrum

In the state with fixed fluxes, operators $\hat{u}_{ij}$ in Hamiltonian (9) can be replaced by corresponding eigenvalues u_{ij} so that Hamiltonian (9) becomes quadratic in the operators of the Majorana fermions. Since each unit cell l in the hexagonal lattice has two vertices $\mathbf{r}_l^A$ and $\mathbf{r}_l^B$, which determine sublattices A and B, Hamiltonian (9) can be written as

$$H = \sum_{\langle l,l'\rangle}\sum_\lambda iM_{ll'}^\lambda c_{A,l}^\lambda c_{B,l'}^\lambda + \sum_{\langle\langle l,l'\rangle\rangle}\sum_{\lambda,\mu} i\tilde{M}_{ll'}^{\lambda\mu}(c_{A,l}^\lambda c_{A,l'}^\mu + c_{B,l}^\lambda c_{B,l'}^\mu), \quad (10)$$

where the first term describes the nearest neighbor hopping of the Majorana fermions with the hopping matrix $\hat{M}$ with elements $M_{ll'}^\lambda = -J_{ij}^\lambda \hat{u}_{ll'}^{AB}$ when vertices $\mathbf{r}_l^A$ and $\mathbf{r}_l^B$ are connected by a bond of type λ (where, for convenience, we have changed the notation for operator from $\hat{u}_{ij}$ to $\hat{u}_{ll'}^{AB}$), otherwise, $M_{ll'} = 0$. The second term in Eq. (10) describes the hopping between next nearest neighbors with matrix

$$\tilde{M}_{ll'}^{\lambda\mu} = -(\kappa\delta_{\lambda\mu} + \eta(1-\delta_{\lambda\mu}))\hat{u}_{ll''}^{AB}\hat{u}_{l'l''}^{AB}.$$

Hamiltonian (10) can be diagonalized in the momentum space if the translation invariance is not violated. Since we can replace all coupling operators in the ground state by their eigenvalues $u^{AB} = 1$, the Hamiltonian in the momentum representation takes form

$$H = \frac{1}{2}\sum_{\mathbf{q}} \mathbf{c}_{-\mathbf{q}}^T iA_{\mathbf{q}}\mathbf{c}_{\mathbf{q}}, \quad (11)$$

where $\mathbf{c}_{\mathbf{q}}^T = (c_{A,\mathbf{q}}^x, c_{A,\mathbf{q}}^y, c_{B,\mathbf{q}}^z, c_{B,\mathbf{q}}^x, c_{B,\mathbf{q}}^y, c_{B,\mathbf{q}}^z)$, and matrix $iA(\mathbf{q})$ has form

$$iA_{\mathbf{q}} = \begin{pmatrix} M_{\mathbf{q}} & F_{\mathbf{q}} & F_{\mathbf{q}} \\ F_{\mathbf{q}} & M_{\mathbf{q}} & F_{\mathbf{q}} \\ F_{\mathbf{q}} & F_{\mathbf{q}} & M_{\mathbf{q}} \end{pmatrix}. \quad (12)$$

In this expression, the following notation has been used:

$$M_{\mathbf{q}} = \begin{pmatrix} \Delta_\kappa(\mathbf{q}) & if(\mathbf{q}) \\ -if^*(\mathbf{q}) & -\Delta_\kappa(\mathbf{q}) \end{pmatrix}, \quad F_{\mathbf{q}} = \begin{pmatrix} \Delta_\eta(\mathbf{q})/2 & 0 \\ 0 & -\Delta_\eta(\mathbf{q})/2 \end{pmatrix}, \quad (13)$$

In the isotropic limit, we have

$$f(\mathbf{q}) = 2J(1 + e^{i\mathbf{q}\cdot\mathbf{n}_1} + e^{i\mathbf{q}\cdot\mathbf{n}_2}),$$

where

$$\mathbf{n}_1 = \left(\frac{\sqrt{3}}{2}, \frac{3}{2}\right),$$

$$\mathbf{n}_2 = \left(-\frac{\sqrt{3}}{2}, \frac{3}{2}\right).$$

Here, the diagonal terms

$$\Delta_\kappa(\mathbf{q}) = 4\kappa(\sin(\mathbf{q}\cdot\mathbf{n}_1) - \sin(\mathbf{q}\cdot\mathbf{n}_2) + \sin(\mathbf{q}\cdot(\mathbf{n}_2 - \mathbf{n}_1))$$

and

$$\Delta_\eta(\mathbf{q}) = 4\eta(\sin(\mathbf{q}\cdot\mathbf{n}_1) - \sin(\mathbf{q}\cdot\mathbf{n}_2) + \sin(\mathbf{q}\cdot(\mathbf{n}_2 - \mathbf{n}_1))$$

describe the hopping between the next nearest neighbors, appearing when TRS is broken.

If $\kappa = \eta = 0$ and TRS is not broken, the Majorana fermion spectrum $\epsilon_{i,\mathbf{q}} = |f(\mathbf{q})|$ contains three degenerate branches, each of which has two Dirac points at the corners $\pm K$ of the Brillouin zone. Once TRS is broken (i.e., $\kappa \neq 0$ or $\eta \neq 0$), at least one of the spectral branches acquires a gap. If $\kappa \neq 0$, but $\eta = 0$, all three spectral branches have a gap, but still remain degenerate. Therefore, when $\eta = 0$, the spectrum in the Yao–Lee model is exactly the three-fold degenerate spectrum of the Kitaev model. If, however, $\eta \neq 0$, the Majorana modes are hybridized with one another, and the degeneracy is partly removed; however, two modes

still remain degenerate (Fig. 2). In this case, the eigenvalues of the perturbed Yao–Lee model (9) are defined as

$$\epsilon_{1,\mathbf{q}} = \pm\sqrt{|f(\mathbf{q})|^2 + (\Delta_\kappa(\mathbf{q}) + \Delta_\eta(\mathbf{q}))^2}, \quad (14)$$

$$\epsilon_{2,\mathbf{q}} = \pm\sqrt{|f(\mathbf{q})|^2 + \left(\Delta_\kappa(\mathbf{q}) - \frac{\Delta_\eta(\mathbf{q})}{2}\right)^2}, \quad (15)$$

$$\epsilon_{3,\mathbf{q}} = \pm\sqrt{|f(\mathbf{q})|^2 + \left(\Delta_\kappa(\mathbf{q}) - \frac{\Delta_\eta(\mathbf{q})}{2}\right)^2}. \quad (16)$$

3. VACANCIES IN THE YAO–LEE MODEL

A vacancy in the lattice is usually just the absence of an atom at a site or at several nearest sites. However, in this study, we will use this term in a wider sense (for example, for describing nonmagnetic impurities or for magnetic atoms that are coupled very weakly with their neighbors). To distinguish between these two cases, the second type of the local defect will be referred to as *quasi-vacancy*.

Let us consider randomly distributed quasi-vacancies in the isotropic Yao–Lee model. For this, we write the first term in the expression (9) as

$$i\sum_{\substack{\langle ij\rangle \\ i,j\in\mathbb{P}}} J\hat{u}_{ij}c_i^\lambda c_j^\lambda + i\sum_{\substack{\langle kl\rangle \\ k\in\mathbb{V},l\in\mathbb{P}}} J'\hat{u}_{kl}c_k^\lambda c_l^\lambda, \quad (17)$$

where $J' \ll J$ determines the interaction of the spin on a defect with the remaining spins of the lattice; $\mathbb{P}$ denotes the set of normal vertices of the lattice, and $\mathbb{V}$ is the set of vertices with quasi-vacancies (see Fig. 1). Further, for simplicity, we will not distinguish between vacancies and quasi-vacancies, presuming that in the limit $J' \ll J$, the vertices belonging to $\mathbb{V}$ behave as quasi-vacancies, while in the limit $J' \to 0$, the vertices become actual vacancies, in which Majorana fermions c_v^α at the vacancy center have zero amplitudes of jumps to neighboring neighbors. We will also consider only the realizations of disorder, for which the number of vacancies in sublattices A and B is the same.

Hamiltonian (10) can still be diagonalized in the presence of vacancies in spite of the fact that the number of degrees of freedom in the limit $J' \to 0$ effectively decreases because three plaquettes are combined into one near each vacancy (the exact solution in the original model exists since the number of spin degrees of freedom is equal to the number of conserved quantities) [25]. The diagonalization of the Hamiltonian can be performed numerically on finite-size clusters with periodic boundary conditions. The diagonalized Hamiltonian has form

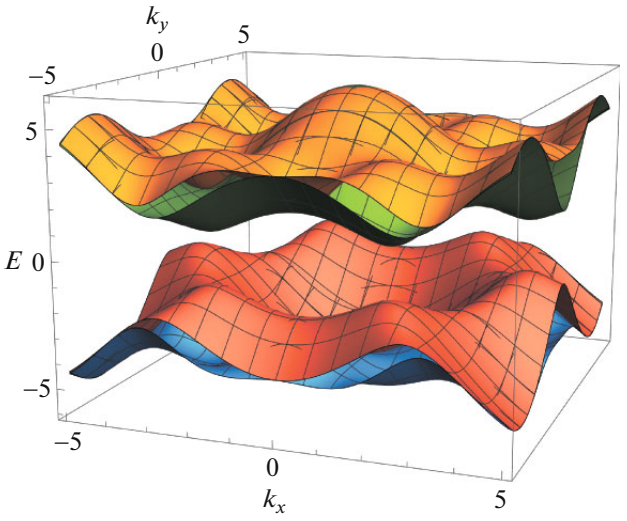

Fig. 2. Spectrum $E(k)$ of the Majorana fermions in the Yao–Lee model [1] with broken TRS (9). The upper spectral branch is nondegenerate and is defined by Eq. (14), while the lower branch is doubly degenerate and is described by Eq. (15). In calculations, we assumed that $\kappa = \eta = 0.2$. All energies are given in the units of J.

$$\mathcal{H} = \sum_n \epsilon_n\left(\psi_n^\dagger\psi_n - \frac{1}{2}\right), \quad (18)$$

where ψ_n are complex fermions. The eigenenergies $\epsilon_n \equiv \epsilon_n(\{J_{ij}\}, \{u_{ij}\})$ can be obtained for each realization of disorder and flux distribution.

3.1. Vacancies with a Bound Flux

The analysis of vacancies in the Kitaev model has revealed the emergence of an eigenmode with an extremely low energy (close to zero) and a wavefunction quasi-localized at the sites of the other sublattice around the vacancy center [21, 22, 25]. Additionally, studies have demonstrated that a vacancy binds the Z2 flux [21, 22]. For the gapped phase of the Kitaev model, this can be shown analytically [21]. For the gapless phase, analytical calculations are impossible, but it has been verified numerically that the flux is attached to a vacancy as before [26].

Let us verify whether this remains true for vacancies in the Yao–Lee model. As mentioned earlier, the ground state in the unperturbed Yao–Lee model has zero flux [1]. To estimate the binding energy between the flux and the vacancy, we have considered two vacancies separated by distance $\sim L/2$, where L is the linear size of the system, one of the vacancies belonging to sublattice A and the other to sublattice B (see

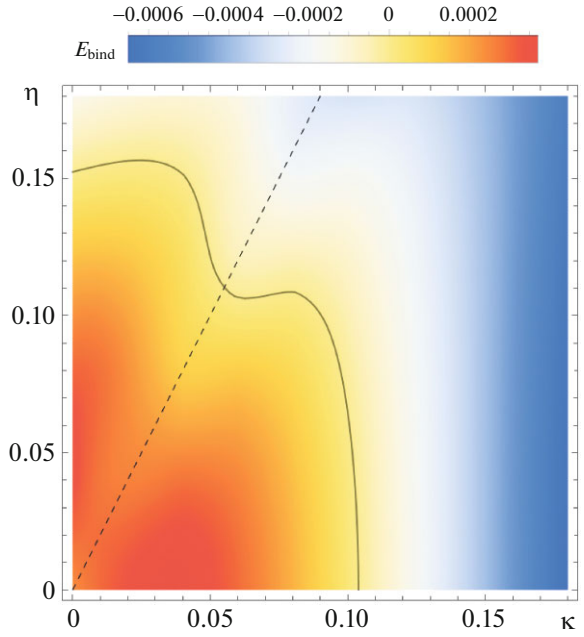

Fig. 3. Dependence of the gain in energy from the attachment of the flux to a vacancy on parameters of Hamiltonian (9), calculated for a finite-size system with $L = 40$. The energy was calculated for a system with two vacancies separated by maximal distance $L/2$. The binding energy and the model parameters are given in the units of J. Dashed line is the straight line on which the gap in two from three branches in the Majorana fermion spectrum is closed. It can easily be seen that the binding energy decreases as this straight line is approached.

Fig. 1). The binding energy is defined by the difference between the energy of the system, in which each vacancy bounds the flux (E_{bound}) and the energy of the system with zero flux (E_{zero}):

$$E_{bind} = \frac{E_{bound} - E_{zero}}{2}. \quad (19)$$

The dependence of the binding energy on parameters κ and η determining the strength of the interactions that break TRS is shown in Fig. 3. It can be seen that with increasing κ and η, a transition occurs from the ground state with the fluxes attached to vacancies to the ground state with zero flux (the line of the transition between the two phases is shown by the solid curve). It should be noted that the existence of a finite density of vacancies can shift the boundary between the phases, but the situation should remain qualitatively unchanged. The binding energy between the flux and a vacancy also decreases as straight line $\kappa = \eta/2$ is approached (dashed line), on which the gap in the spectrum of two from three Majorana bands closes.

3.2. Density of States and IPR

In this section, we discuss how the presence of vacancies affects the low-energy density of states of the Majorana fermions in the Yao–Lee model. The density of states is defined as

$$n(E) = \left\langle \sum_n \delta(E - \epsilon_n) \right\rangle, \quad (20)$$

where the averaging is performed over the independent realizations of disorder. Since the density of states contains information only on the spectrum of the system, but not on the degree of localization of states in the spectrum, we have also calculated the inverse participation ratio (IPR) describing the measure of localization of each state. The IPR is defined as

$$\mathcal{P}_n = \sum_i |\phi_{n,i}|^4, \quad (21)$$

where subscript n labels the wavefunctions $\phi_{n,i}$ of states, while index i labels the sites on the lattice. For a delocalized mode, IPR varies upon an increase in size N of the system as $\sim 1/N$ because the probability density is distributed over the lattice almost uniformly. If, however, the state is localized, its IPR is independent of the size of the system because it is determined only by the probability on a finite number of sites [26].

Figure 4 shows the density of states $n(E)$ in the presence of 2% of vacancies. Figure 4a shows $n(E)$ for a system with unbroken TRS ($\kappa = \eta = 0$), in which a flux is bound to each vacancy, $W_v = -1$, but $W_p = 1$ at all other plaquettes, and the flux is zero. Figures 4b and 4e show $n(E)$ for a system with broken TRS ($\kappa = \eta = 0.2$), in the bound and zero flux sectors, respectively. Figures 4d and 4f show the same densities of states, but only for low energies.

To construct various realizations of disorder with bound flux, we have used the algorithm proposed in [25]; namely, each pair of vacancies to which the flux is attached is formed as follows: (i) a pair of vacancies with a common edge is arranged at random in the system; (ii) the sign of variable u_{ij} at one of common edges changes from $u = +1$ to $u = -1$ so that two fluxes attached to two vacancion plaquettes are created; (iii) one of the vacancies moves at random and, simultaneously, the chain of variables u_{ij} changes sign so that the fluxes are always attached to the moving vacancy, and the fluxes through other cells remain unchanged.

Irrespectively to the flux sector, vacancies induce low-energy states leading to the formation of a peak in the density of states near zero energy. The width of this low-energy peak is determined by the value of exchange interaction $J' = 0.01$, which leads to hybridization of zeroth modes induced by vacancies with the remaining states of the system. It can be seen that even with unbroken TRS (i.e., in the absence of the gap in the spectrum), the states contributing to this peak are quite localized (this can be seen from higher values of IPR in Fig. 4c, indicating the low-energy part of $n(E)$ in Fig. 4a). It should be noted that for $\kappa = \eta = 0$, each

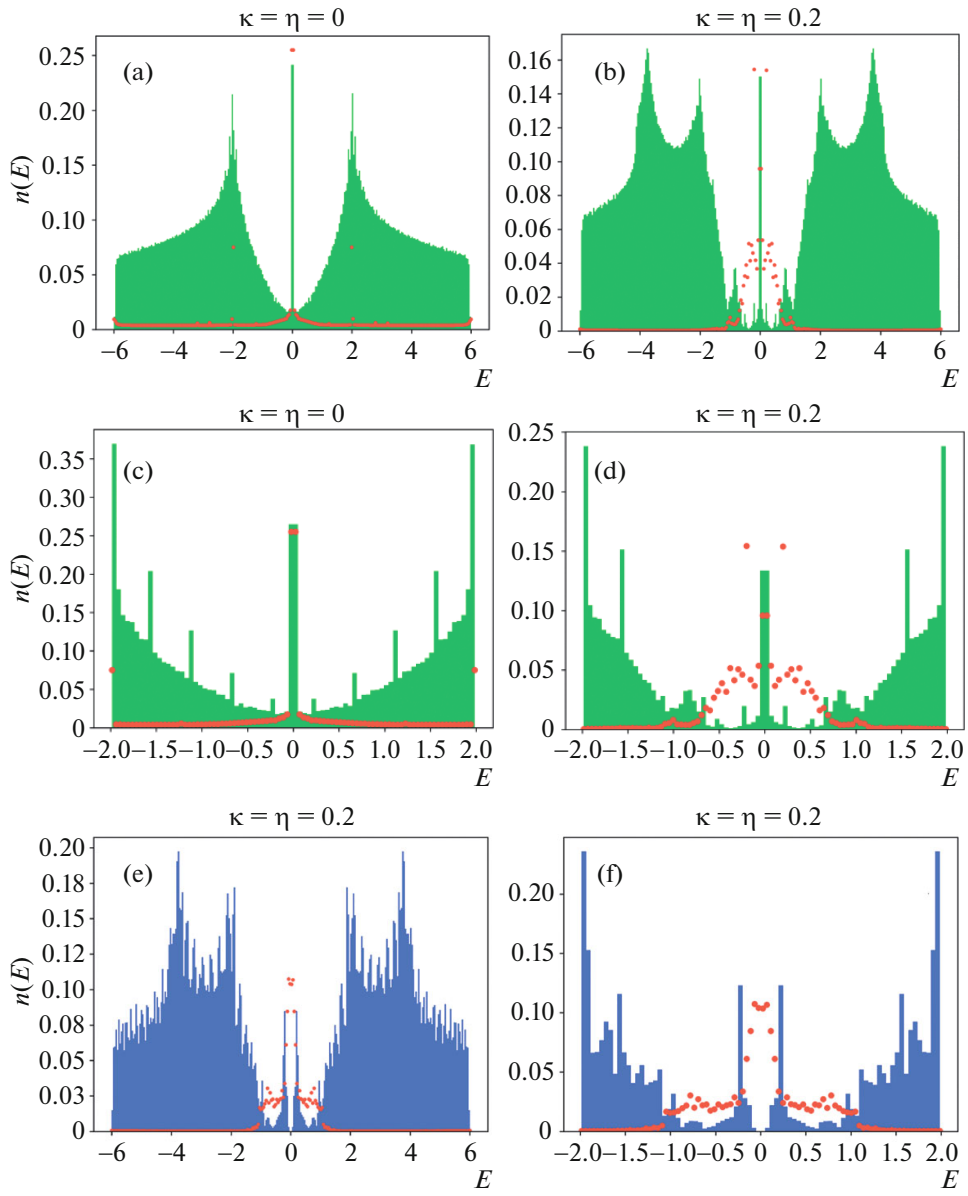

Fig. 4. Density of states $n(E)$ in the Yao–Lee model in the presence of 2% of vacancies. (a, b) Densities of states $n(E)$ for a system, in which a flux ($W_v = -1$) is attached to each vacancy, are calculated for $\kappa = \eta = 0$ and $\kappa = \eta = 0.2$, respectively. (c, d) The same densities of states, but only for low energies. The width of the low-energy peak is determined by the exchange interaction $J' = 0.01$, which leads to hybridization of zero modes induced by vacancies with the remaining eigenstates of the system. (e) Density of states $n(E)$ in a system with a nonzero flux (all $W_v = 1$ and all $W_p = 1$), calculated for $\kappa = \eta = 0.2$. (f) The same density of states, but only for low energies. Numerical calculations were performed for a finite system with $L = 40$ using periodic boundary conditions. All results were averaged over 40 random realizations. Red bullets correspond to the values of IPR shown on the same scale as $n(E)$ (IPR is multiplied by 4 in (a) and (c)). All energies are given in the units of J.

vacancy in the Yao–Lee model generates two types of tree-fold degenerate low-energy states. Like in the Kitaev model with vacancies [25], the first type of bound states is localized exactly at the vacant vertex that is weakly coupled by J' with their neighbors. The other type of states is localized at the plaquette periphery around the vacancy, at the sites of the other sublattice.

The distinctions between the zero and bound flux sectors become apparent when TRS is broken, giving rise to a gap in the Majorana spectrum. If the gap is sufficiently large (i.e., parameters $\varkappa$ and η determining the gap width are large enough), the spectrum can be effectively described

by the hybridization of in-gap states localized at the same vacancy. Additional weak hybridization occurs

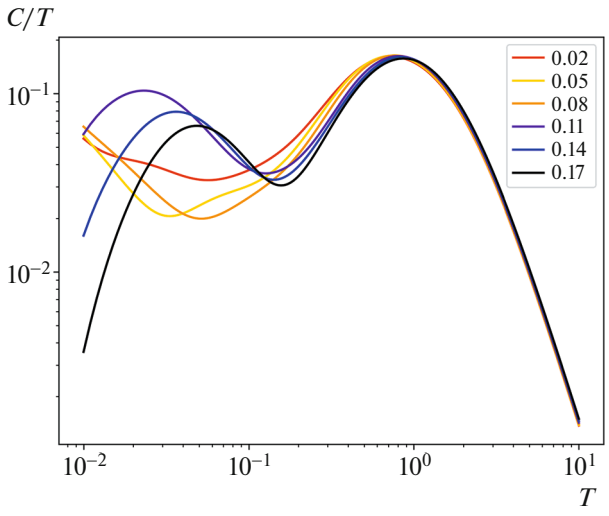

Fig. 5. Temperature dependences of C/T on T (on logarithmic scale) for different values of $\kappa = \eta$, each of which is shown by its own color. Numerical values of T, κ, η, and $J = 0.01$ are given in the units of J. All calculations were performed for 2% of vacancies.

occurs between in-gap states at different vacancies, resulting in an increased width of the in-gap peaks as the density of vacancies increases. Furthermore, a comparison of Figs. 4d and 4f reveals that the structure of in-gap states, especially the number of peaks within the gap, is influenced by the flux through the vacancies. In the case of zero flux, two broad peaks emerge within the gap at finite energies, and the peak near zero vanishes. In the presence of bound flux, additional states emerge, forming a peak in the density of states near zero energy. When vacancies are far from each other and inter-vacancy hybridization is vanishingly small, these states manifest as Majorana zero modes, akin to excitations with anionic statics [36].

Although such a behavior resembles the situation in the Kitaev model [25], it's crucial to note that each vacancy in the Yao–Lee model generates three times as many states compared to the Kitaev model. In addition, the existence of additional TRS breaking term $\eta \neq 0$, changes the very structure of in-gap states. In the general case, the number of resonance peaks in the gap corresponds to the number of localized modes near each vacancy, and the structure of peaks depends on their hybridization.

3.3. Effect of Vacancies on Thermodynamics

Let us consider the effect of vacancies on low-temperature heat-capacity. If the temperature is lower than the energy of flux excitation on the hexagonal plaquette, we can assume that all fluxes are fixed. In this case, the contribution to the heat capacity comes only from the free Majorana fermions,

$$C(T) = \int E \cdot n(E) \cdot \frac{\partial n_F(E,T)}{\partial T} dE = \sum_n \left(\frac{\epsilon_n}{T}\right)^2 \frac{e^{\epsilon_n/T}}{(e^{\epsilon_n/T}+1)^2}, \quad (22)$$

where $n_F(E, T) = (e^{E/T} + 1)^{-1}$ is the Fermi function and $n(E)$ is the density of states.

Figure 5 shows the temperature dependences of C/T (on the logarithmic scale) for different values of $\kappa = \eta \in [0.02, 0.17]$. A transition from the phase with bound fluxes to the phase with zero fluxes occurring approximately for $\kappa = \eta \simeq 0.1$ (see Fig. 3) can be seen from the change in the behavior of the heat capacity. If the system is in the bound flux phase (i.e., for $\kappa = \eta < 0.1$), C/T exhibits the power-law divergence at low temperatures, which appears due to the peak existing in the density of states near zero energy. In the zero flux phase, (i.e., for $\kappa = \eta > 0.1$), the value of C/T tends to zero at temperatures tending to zero. In the latter case, the heat capacity at finite temperatures has a broad peak reflecting the existence of state inside the gap, overall showing a two-hump structure.

4. CONCLUSIONS

In this work, we have studied the effects of disorder and localization in a 2D QSL realized in the exactly solvable Yao–Lee model [1]. It is shown that the presence of vacancies in this model leads to the formation of a peak in the density of states at low energies, which is manifested, for example, in the behavior of the low-temperature heat capacity. In spite of the fact that the low-energy part of the spectrum depends on specific model parameters such as the type of interactions breaking TRS, these states are more localized than other states of the system. The effect of localization has been analyzed numerically using the inverse participation ratio (IPR); it is shown that the localization of low-energy states is manifested especially strongly when each vacancy has a nonzero flux attached to it, and there is a field breaking the time inversion symmetry. If, however, this field is strong enough, it is more advantageous energetically to have zero flux through all plaquettes; however, the localization becomes weaker in this case. It is interesting to note that low-energy states in the gap with broken TRS are an example of a network of quasi-localized Majorana states, which can be used in quantum computations.

ACKNOWLEDGMENTS

The authors are grateful to Wen-Han Kao for cooperation in previous studies, the ideas of which have been used in this work. Thanks are also due to A. Tsvelik for fruitful discussion concerning the Yao–Lee model.

FUNDING

N.B.P. is grateful to the National Science Foundation (award no. DMR-2310318) for partial financial support.

CONFLICT OF INTEREST

The authors of this work declare that they have no conflicts of interest.

ADDITIONAL INFORMATION

This article is prepared for the memorial issue of the journal dedicated to the 95th birthday of L.A. Prozorova.

REFERENCES

1. H. Yao and D.-H. Lee, Phys. Rev. Lett. **107**, 087205 (2011).
2. W. Witczak-Krempa, G. Chen, Y. B. Kim, and L. Balents, Ann. Rev. Condens. Matter Phys. **5**, 57 (2014).
3. C. L. Kane and E. J. Mele, Phys. Rev. Lett. **95**, 146802 (2005).
4. B. A. Bernevig and S.-C. Zhang, Phys. Rev. Lett. **96**, 106802 (2006).
5. R. Moessner and J. E. Moore, *Topological Phases of Matter* (Cambridge Univ. Press, Cambridge, 2021).
6. P. W. Anderson, Mater. Res. Bull. **8**, 153 (1973).
7. L. Balents, Nature (London, U.K.) **464**, 199 (2010).
8. L. Savary and L. Balents, Rep. Prog. Phys. **80**, 016502 (2017).
9. M. R. Norman, Rev. Mod. Phys. **88**, 041002 (2016).
10. J. Knolle and R. Moessner, Ann. Rev. Condens. Matter Phys. **10**, 451 (2019).
11. C. Broholm, R. J. Cava, S. A. Kivelson, D. G. Nocera, M. R. Norman, and T. Senthil, Science (Washington, DC, U. S.) **367**, eaay0668 (2020).
12. H. Takagi, T. Takayama, G. Jackeli, G. Khaliullin, and S. E. Nagler, Nat. Rev. Phys. **1**, 264 (2019).
13. A. Kitaev, Ann. Phys. **321**, 2 (2006).
14. H. Yao, S.-C. Zhang, and S. A. Kivelson, Phys. Rev. Lett. **102**, 217202 (2009).
15. F. Wang and A. Vishwanath, Phys. Rev. B **80**, 064413 (2009).
16. C. Wu, D. Arovas, and H.-H. Hung, Phys. Rev. B **79**, 134427 (2009).
17. R. Nakai, S. Ryu, and A. Furusaki, Phys. Rev. B **85**, 155119 (2012).
18. V. S. de Carvalho, H. Freire, E. Miranda, and R. G. Pereira, Phys. Rev. B **98**, 155105 (2018).
19. G. Jackeli and G. Khaliullin, Phys. Rev. Lett. **102**, 017205 (2009).
20. J. Chaloupka, G. Jackeli, and G. Khaliullin, Phys. Rev. Lett. **105**, 027204 (2010).
21. A. J. Willans, J. T. Chalker, and R. Moessner, Phys. Rev. Lett. **104**, 237203 (2010).
22. A. J. Willans, J. T. Chalker, and R. Moessner, Phys. Rev. B **84**, 115146 (2011).
23. J. Knolle, R. Moessner, and N. B. Perkins, Phys. Rev. Lett. **122**, 047202 (2019).
24. J. Nasu and Y. Motome, Phys. Rev. B **102**, 054437 (2020).
25. W.-H. Kao, J. Knolle, G. B. Halasz, R. Moessner, and N. B. Perkins, Phys. Rev. X **11**, 011034 (2021).
26. W.-H. Kao and N. B. Perkins, Ann. Phys. **435**, 168506 (2021).
27. W.-H. Kao and N. B. Perkins, Phys. Rev. B **106**, L100402 (2022).
28. V. Dantas and E. C. Andrade, Phys. Rev. Lett. **129**, 037204 (2022).
29. P. W. Anderson, Phys. Rev. **109**, 1492 (1958).
30. I. M. Lifshitz, Sov. Phys. Usp. **7**, 549 (1965).
31. A. Y. Kitaev, Phys. Usp. **44**, 131 (2001).
32. C. Nayak, S. H. Simon, A. Stern, M. Freedman, and S. Das Sarma, Rev. Mod. Phys. **80**, 1083 (2008).
33. J. D. Sau, S. Tewari, R. M. Lutchyn, T. D. Stanescu, and S. Das Sarma, Phys. Rev. B **82**, 214509 (2010).
34. R. R. Biswas, Phys. Rev. Lett. **111**, 136401 (2013).
35. K. Damle, Phys. Rev. B **105**, 235118 (2022).
36. D. A. Ivanov, Phys. Rev. Lett. **86**, 268 (2001).
37. S. Tewari, S. Das Sarma, and D.-H. Lee, Phys. Rev. Lett. **99**, 037001 (2007).
38. V. Gurarie and L. Radzihovsky, Phys. Rev. B **75**, 212509 (2007).
39. R. Roy, Phys. Rev. Lett. **105**, 186401 (2010).
40. C. Xu, J. Feng, M. Kawamura, Y. Yamaji, Y. Nahas, S. Prokhorenko, Y. Qi, H. Xiang, and L. Bellaiche, Phys. Rev. Lett. **124**, 087205 (2020).
41. E. H. Lieb, Phys. Rev. Lett. **73**, 2158 (1994).

Translated by N. Wadhwa